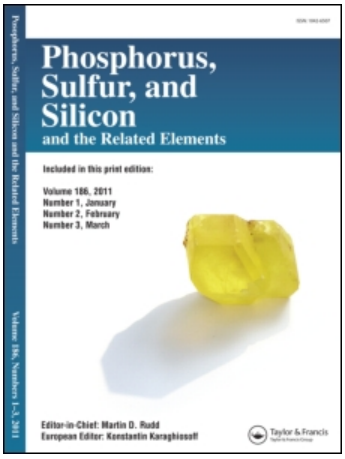

Phosphorus, Sulfur, and Silicon and the Related Elements

Publication details, including instructions for authors and subscription information:
http://www.informaworld.com/smpp/title~content=t713618290

Crystal Structure and Investigation of An Organic Phosphate

H. Dhaouadi[a]; H. Marouani[a]; M. Rzaigui[a]; A. Madani[b]
[a] Laboratoire de Chimie des Matériaux, Faculté des Sciences, Zarzouna, Bizerte, Tunisie [b] Laboratoire de Physique des Matériaux, Faculté des Sciences, Zarzouna, Bizerte, Tunisie

To cite this Article Dhaouadi, H. , Marouani, H. , Rzaigui, M. and Madani, A.(2007) 'Crystal Structure and Investigation of An Organic Phosphate', Phosphorus, Sulfur, and Silicon and the Related Elements, 182: 11, 2587 — 2603
To link to this Article: DOI: 10.1080/10426500701512026
URL: http://dx.doi.org/10.1080/10426500701512026

Phosphorus, Sulfur, and Silicon, 182:2587–2603, 2007

ISSN: 1042-6507 print / 1563-5325 online
DOI: 10.1080/10426500701512026

Taylor & Francis
Taylor & Francis Group

Crystal Structure and Investigation of An Organic Phosphate

H. Dhaouadi
H. Marouani
M. Rzaigui
Laboratoire de Chimie des Matériaux, Faculté des Sciences, Zarzouna, Bizerte, Tunisie

A. Madani
Laboratoire de Physique des Matériaux, Faculté des Sciences, Zarzouna, Bizerte, Tunisie

The crystal structure of (6-$NH_2C_5H_3NHCO_2H$)H_2PO_4 was determined by X-ray diffraction on single crystal. The crystal symmetry is triclinic $P\bar{1}$ with unit cell dimensions $a = 7.221(1)$ Å, $b = 8.086(2)$ Å, $c = 8.832(5)$ Å, $\alpha = 81.97(8)^\circ$, $\beta = 100.52(8)^\circ$, $\gamma = 116.32(6)^\circ$, $V = 453.4(4)$ Å^3 and $Z = 2$. The crystal structure has been solved and refined down to $R = 0.030$ and $R_w = 0.050$, using 4129 independent reflections. The atomic arrangement contains inorganic layers parallel to the ab plane around $z = 1/2$. The organic groups, (6-$NH_2C_5H_3NHCO_2H$)$^+$, are anchored between adjacent polyanions through multiple hydrogen bonds. Geometrical characteristics of the hydrogen bonds are described. Electrical conductivity measurements show that the (6-$NH_2C_5H_3NHCO_2H$)H_2PO_4 has a conductivity value $\sigma = 7.1\ 10^{-6}\Omega^{-1}cm^{-1}$ at 318 K with an activation energy $E_a = 0.11$ eV.

Keywords crystal structure; dihydrogenphosphate; Electric conductivity; Hybrid compound; NMR spectroscopy; X-ray diffraction

INTRODUCTION

The combination of organic molecules and inorganic materials was the starting point for the development of new hybrid compounds with desired physical and chemical properties.[1] These materials have raised widespread interest, due to their exceptional opportunity to combine the remarkable features of organic molecules with those of inorganic

Received March 31, 2007; accepted May 4, 2007.
Address correspondence to Houda Marouani, Laboratoire de chimie des Matériaux, Faculté des Sciences, 7021 Zarzouna, Bizerte, Tunisie. E-mail: houda.marouani@fsb.rnu.tn

materials. Among the varieties of explored hybrid compounds, organic phosphates are particularly interesting. Their applications have been explored and reported in various fields, such as magnetism, electricity and optics.[2] Designing these hybrid materials is highly influenced by several factors, such as the nature and the shape of the organic molecule.

In order to enrich the varieties in such kinds of hybrid materials and to investigate the influence of hydrogen bonds on the chemical and structural features, we report and discuss the chemical preparation and the structural investigation of a new organic monophosphate (6-$NH_2C_5H_3NHCO_2H)H_2PO_4$ in this article. From this viewpoint, the 6-aminonicotinic acid, (6-$NH_2C_5H_3NCO_2H$), is considered to be suitable for the present work. It can act as a hydrogen-bond acceptor but also as a hydrogen-bond donor, inducing many rich interesting structures with higher dimensions. The title compound has also been characterized by IR, NMR, DTA/TGA, and impedance spectroscopy.

RESULTS AND DISCUSSION

Crystal Structure

The formula unit, (6-$NH_2C_5H_3NHCO_2H)H_2PO_4$, corresponds to the asymmetric unit in this structure. The configuration of its components is shown in Figure 1. Main geometrical features of the different entities are reported in Table I.

The unit cell projection along the a axis (Figure 2) shows that the $H_2PO_4^-$ tetrahedra are connected by strong hydrogen bonds of O–H···O type, forming centrosymmetric dimers of the formula $[H_4P_2O_8]^{2-}$. Both hydrogen atoms, H(O1) (0, 0, ½) and H(O2) (½, 0, ½), occupy the inversion centres (0, 0, ½) and (½, 0, ½), respectively. In these positions, the hydrogen atoms perform strong symmetrical bonds O···H···O, with distances O···O = 2.466(3) Å and 2.449(2) Å. Each of the hydrogen atoms H(O1) and H(O2) is centered between two identical anions, $H_2PO_4^-$, with O1···H(O1) = H(O1)···O1 = 1.233(1) Å and O2···H(O2) = H(O2)···O2 = 1.224(1) Å (Table II), thus producing a two-dimensional anionic network. Similar strong symmetrical hydrogen bonds are found in crystals of other hydrogenphosphates such as $CaHPO_4$,[3] $CsMnHP_3O_{10}$,[4] and $RbMnHP_3O_{10}$.[5]

The calculated average values of the distortion indices [6] corresponding to the different angles and distances in the independent PO_4 tetrahedron, DI(PO) = 0.013, DI(OPO) = 0.021, and DI (OO) = 0.007 show a pronounced distortion of the OPO angles and PO distances if compared to OO distances. So the phosphate group can be considered as a

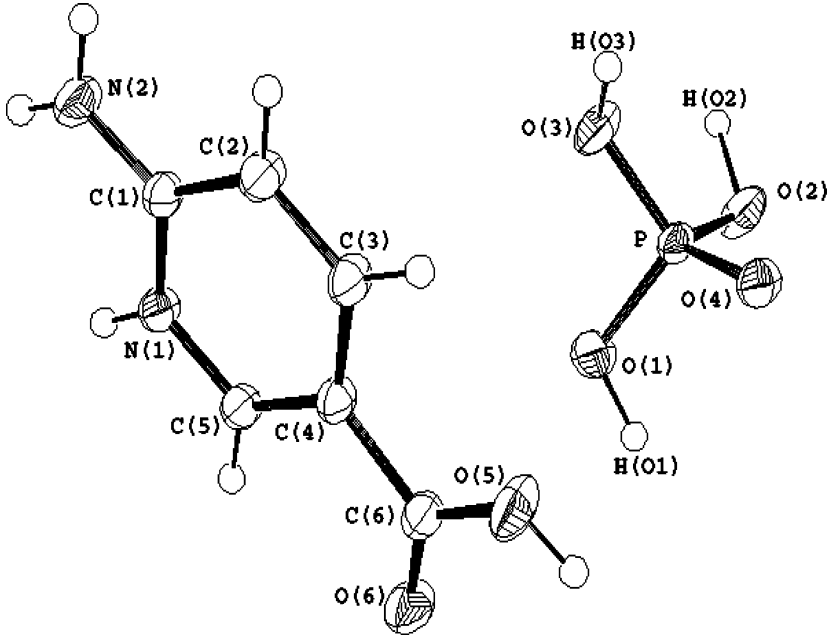

FIGURE 1 ORTEP view of the formula unit of (6-$NH_2C_5H_3NHCO_2H$)H_2PO_4 (50% thermal ellipsoids).

rigid regular tetrahedral arrangement of oxygen atoms where P atom is slightly shifted from the gravity centre. We note that the distance between the phosphorus atom and the oxygen atoms bearing the hydrogen atom (P-OH) is the longest one. This is in accordance with all that has been previously observed for PO_4 tetrahedra involved in dihydrogenphosphate anions.[7]

With regards to the organic cation arrangement, infinite chains of [6-$NH_2C_5H_3NH^+CO_2H$] cations spread along the b direction (Figure 3). These organic chains are connected to the inorganic layer through short H-bonds: N—H···O and O—H···O. The role of organic cations is to organise the anionic aggregates in layers or chains of various typical geometries following the position and the number of functional groups, which are hydrogen donors and acceptors. The average of the C—N distances in pyridine ring is 1.355 Å and of C—C is 1.380 Å. These last values are in the same order of those of non-substituted pyridine and may indicate some aromatic bond character.[8] The C(1)—N(2) bond is 1.326 (1) Å and is approximately equal to C=N double bond length, indicating that the atom N(2) of the amino group must be sp^2hybridized. This also is supported by the C(1)—N(2)—H(6) angle of 125.6 (8)° and

TABLE I Main Interatomic Distances (Å) and Angles (°) in $(6\text{-}NH_2C_5H_3NHCO_2H)H_2PO_4$ Atomic Arrangement. Estimated Standard Deviations are Given in Parentheses

The PO_4 tetrahedron				
P	O(1)	O(2)	O(3)	O(4)
O(1)	**1.545(1)**	2.498(1)	2.509(3)	2.504(2)
O(2)	108.78(7)	**1.528(1)**	2.554(3)	2.547(2)
O(3)	107.51(9)	104.91(6)	**1.567(2)**	2.523(2)
O(4)	110.49(7)	114.31(7)	110.50(7)	**1.503(2)**
O(1)-H(O1)	1.233(1)	P-O(1)-H(O1)		119.81(7)
O(2)-H(O2)	1.224(1)	P-O(2)-H(O2)		118.08(8)
O(3)-H(O3)	0.99(2)	P-O(3)-H(O3)		111.00(1)
$(6\text{-}NH_2C_5H_3NHCO_2H)^+$ group				
N(1)-C(1)	1.355(1)	N(1)-C(1)-N(2)		119.11(7)
C(1)-C(2)	1.418(1)	N(1)-C(1)-C(2)		118.11(8)
C(2)-C(3)	1.368(1)	C(1)-C(2)-C(3)		119.79(9)
C(3)-C(4)	1.413(1)	C(2)-C(3)-C(4)		120.30(7)
C(4)-C(5)	1.325(1)	C(4)-C(5)-N(1)		121.06(9)
N(2)-C(1)	1.326(1)	C(5)-N(1)-C(1)		122.41(6)
C(4)-C(6)	1.480(1)	C(5)-C(4)-C(6)		117.89(9)
C(6)-O(6)	1.216(1)	C(3)-C(4)-C(6)		123.80(7)
C(6)-O(5)	1.307(1)	C(4)-C(6)-O(5)		113.55(9)
C(5)-N(1)	1.355(1)	C(4)-C(6)-O(6)		122.38(7)
O(5)-H(9)	0.90(2)	C(3)-C(4)-C(5)		118.30(9)
N(2)-C(1)-C(2)	122.77(9)	O(5)-C(6)-O(6)		124.06(9)
Hydrogen—bond				
D—H···A	D···A	D—H	H···A	D—H···A
O1···H(O1)···O1	2.466(3)	1.233(1)	1.233(1)	180.0
O2···H (O2)···O2	2.449(2)	1.224(1)	1.224(1)	180.0
O3—H(O3)···O(4)	2.583(1)	0.99(2)	1.60(2)	170(1)
O5—H(O5)···O(1)	2.641(2)	0.90(2)	1.74(6)	177(6)
N1—H(N1)···O(4)	2.678(2)	0.91(2)	1.80(2)	159(1)
N2—H(1N2)···O(2)	2.853(2)	0.87(1)	1.99(1)	169(1)
N2—H(2N2)···O(6)	2.863(3)	0.90(1)	1.99(1)	162(1)

TABLE II Bond Lengths (Å) and Angles (°) in the Hydrogen–Bonding Scheme of $(o\text{–}NH_2C_5H_3NH)H_2PO_4$

D—H···A	D···A	D—H	H···A	D—H···A
O(1)···H(O1)···O(1)	2.470(2)	1.24	1.24	180.0
O(3)···H(O3)···O(3)	2.467(2)	1.23	1.23	180.0
O(2)—H(O2)···O(4)	2.585(1)	0.89	1.70	178.0
N(1)—H(1N1)···O(1)	2.738(1)	0.93	1.81	171.7
N(2)—H(1N2)···O(4)	2.908(2)	0.71	2.24	157.6
N(2)—H(2N2)···O(3)	2.979(2)	1.00	1.99	173.8

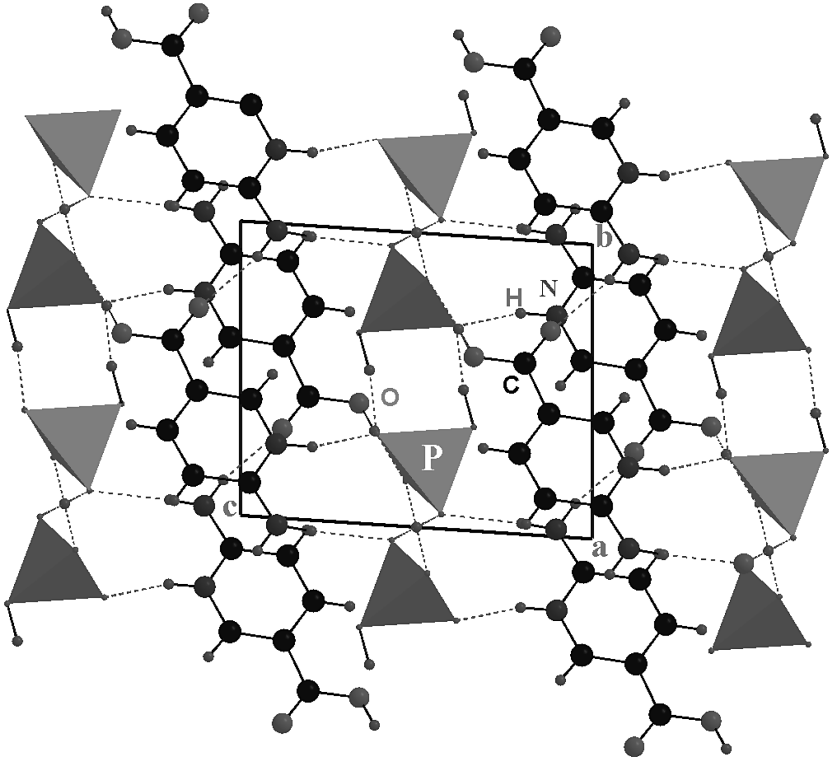

FIGURE 2 The atomic arrangement of $(6\text{-}NH_2C_5H_3NHCO_2H)H_2PO_4$in projection along the a-axis. The phosphoric groups are given in tetrahedral representation. The other atoms are indicated by their symbols. Intermolecular H-bonds are denoted by dotted lines.

by the fact that the atoms C(1), N(2), H(5) and H(6) lie almost in the pyridine plane. The pyridine ring displays an almost coplanar configuration, with a mean plane deviation of 0.0047 Å. The interplanar distance between the rings of the organic cations is in the vicinity of 3.72 Å, indicating the formation of $\pi - \pi$ interactions.[9]

The carboxylic acid group (—CO_2H) is planar, and lies in the plane of the pyridine ring. This coplanarity can be seen from the torsion angle values of [O(6)—C(6)—C(4)—C(5)] = 3.7(1)°, and [O(6)—C(6)—C(4)—C(3)] = −176.98(7)°. The C(3)—C(4)—C(6) angle (123.8°) is larger than the C(5)—C(4)—C(6) one (117.9°). This effect can be attributed to the establishment of a weak intramolecular hydrogen bond [C(5)—H···O(6) = 97.05°, C(5)···O(6) = 2.777 Å, H···O(6) = 2.496 Å]. The formation of this kind of intramolecular hydrogen bonds would allow the organic molecule to be highly planar.

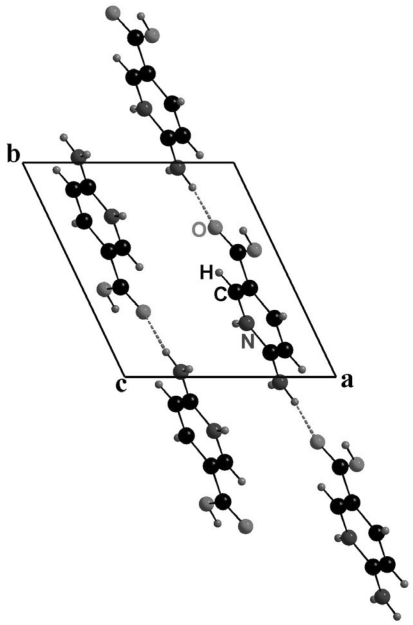

FIGURE 3 The organic cations arrangement of $(6\text{-}NH_2C_5H_3NHCO_2H)H_2PO_4$.

A comparison of the title compound (I) to 2-aminopyridinium dihydrogenmonophosphate (II)[10] shows that they differ only by the nature of the substituents on the pyridine ring.

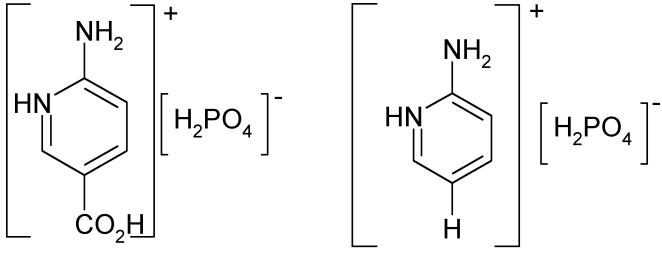

(I) (II)

The structure of (I) is quite different from that of $(2\text{-}NH_2C_5H_3NH)H_2PO_4$ (II), which contains a three-dimensional network of $H_2PO_4^-$ groups encapsulating the organic moieties in space group C2/c. The three-dimensional network seems to be as cohesive as the two-dimensional network of (I), as confirmed by the values of hydrogen bonds in both anionic aggregates. Although the connectivity of the dihydrogenphosphate tetrahedra is completely different, both compounds (I) and (II) contain three similar N—H···O interactions [for (I), mean

H···O = 1.93 Å and mean N···O = 2.798 Å, for (II) mean H···O = 2.03 Å and mean N···O = 2.875 Å] (Table II). It is worth-noting that $\pi - \pi$ interactions between pyridine rings, stacked in opposition, are more prevalent in the second structure ($d_{II} = 3.51 < d_I = 3.72$ Å).

In contrast to the two-dimensional structure of (I), and to the three-dimensional structure of (II), the structure of (2-NH_2-6-CH_3-$C_5H_3NH)H_2PO_4$(III)[11] may be described as infinite chains composed of H2PO4$^-$ groups. These chains cross the unit cell at x = $^1/_2$ parallel to the b direction. If compared to structure (I), the attraction between (2 - NH2 - 6 - CH3 - C5H3NH)$^+$ cations and $[H2PO4]_n^{n-}$ layers is thus more important than that observed between (6 - NH2C5H3NH$^+$ CO2H) and $[H2PO4]_n^{n-}$ layers. This situation is clearly evidenced by comparison of the N—H···O contacts in both structures [for (I), mean N···O = 2.798 Å, for (III) mean N···O = 2.633 Å].

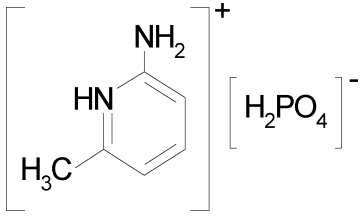

(III)

For these three compounds, these results allow us to conclude that the structure of the organic monophosphates is highly influenced by the nature and the position of the substituents on the pyridine ring.

NMR Results

High resolution NMR spectroscopy is a powerful technique for the characterization of phosphates. From the isotropic chemical shift values of NMR components, structural aspects have been studied. Proton decoupled ^{31}P MAS – NMR spectrum of crystalline monophosphate (6-$NH_2C_5H_3NHCO_2H)H_2PO_4$is presented in Figure 4. It exhibits only one sharp peak. The corresponding chemical shift value (0.29 ppm) was recorded with respect to 85% H_3PO_4 aqueous solution. This chemical shift value agrees with those of monophosphate (between −10 and +5 ppm), depending on the compound.[12–17]The single isotropic peak observed is related to the number of phosphorus sites, which exist in the unit cell of the compound structure.

Figure 5 shows the ^{13}C NMR spectra of (6-$NH_2C_5H_3NHCO_2H)H_2PO_4$ recorded in solid-state and D_2O solution. The calculated and experimental chemical shifts for ^{13}C carbon atoms are displayed in Table III. As expected, the chemical shifts for aromatic carbons are located in

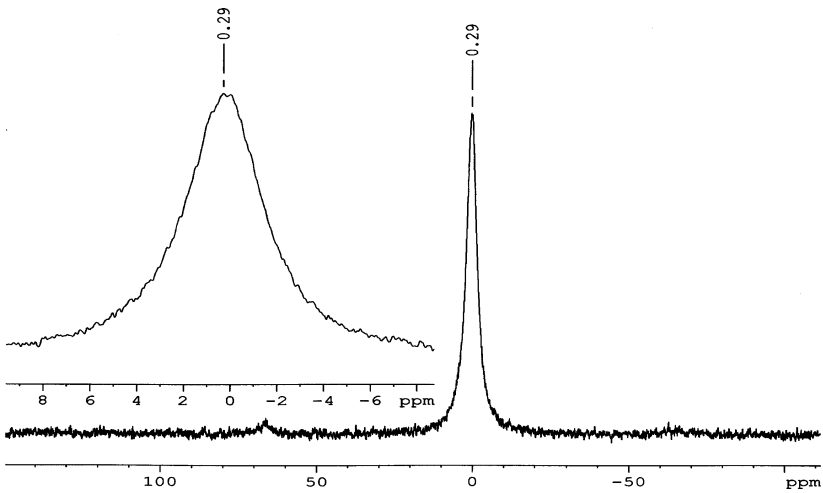

FIGURE 4 ^{31}P MAS-NMR spectrum of $(6\text{-}NH_2C_5H_3NHCO_2H)H_2PO_4$.

the range 107–161 ppm. It is important to note that the chemical shift value of the C6 carbon atom ($\delta = 166.8$ ppm) is higher than those of the aromatic ring. This can be explained by the electronegativity effect of the two oxygen atoms O5 and O6. Theoretical chemical shifts have been performed with Chem-Drew Ultra 6.0 calculations. The two spectra display six resonance peaks corresponding to different carbon atoms of the organic group which are labelled as depicted below. The two spectra exhibit comparable chemical shifts, the difference between solution-solid chemical shifts usually results from the changes in molecular geometry and intermolecular interactions.

A correlation between experimental ^{13}C (CPMAS) chemical shifts versus chemical shifts in the D_2O solution is satisfactory ($R^2 = 0.9956$), as seen in Figure 6. This may be explained by the fact that the carbon atoms are not involved in intermolecular hydrogen bonds of C—H···O type, which is confirmed by X-ray crystallography.

These results are in good agreement with the X-ray structure as only one organic molecule is found in the asymmetric unit.

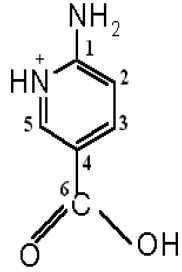

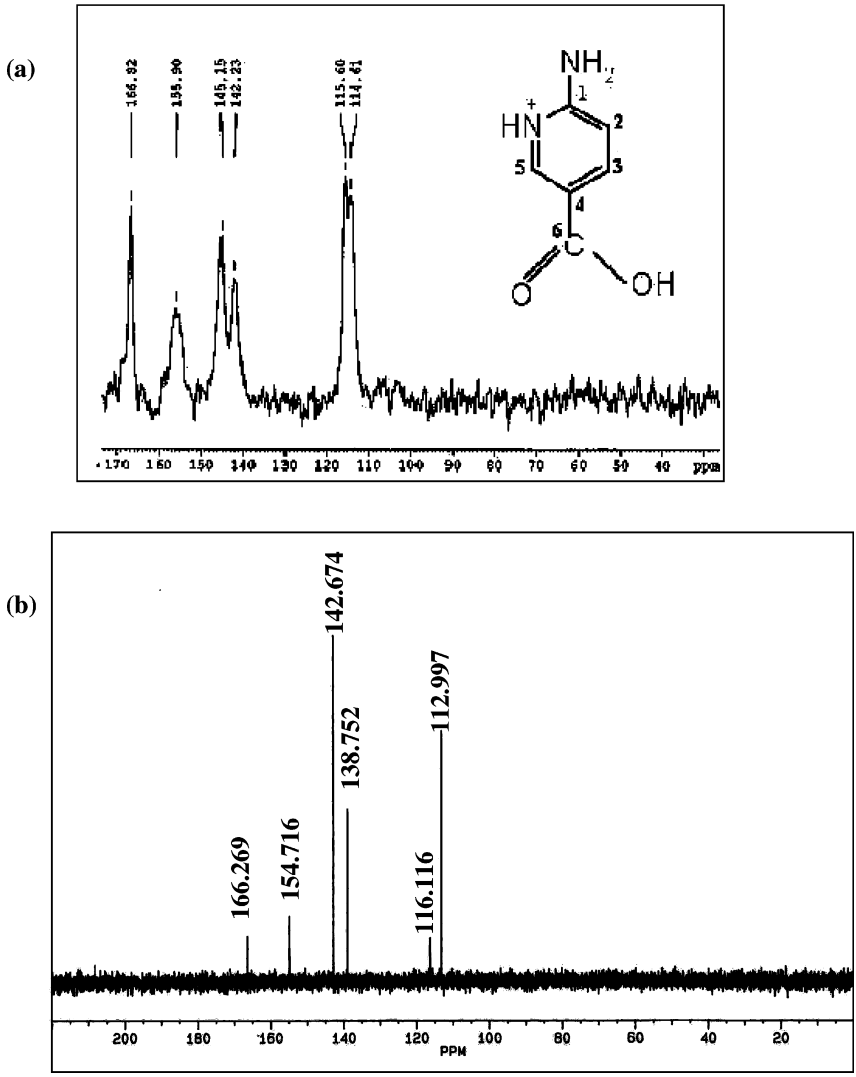

FIGURE 5 (a) ^{13}C CP MAS-NMR spectra of $(6\text{-}NH_2C_5H_3NHCO_2H)H_2PO_4$ in the solid state; and (b) D_2O solution.

Thermal Analysis

Figure 7 shows the TGA and DTA thermograms of the title compound in the temperature range [20 to 450°C]. The DTA curve shows that the monophosphate is stable until 226°C, where it undergoes a melting transformation**,** with which occurs simultaneously a decomposition

TABLE III ^{13}C NMR Chemical Shifts for (6-$NH_2C_5H_3NHCO_2H$)H_2PO_4 in the Solid-State and D_2O Solution

Carbon atoms	C1	C2	C3	C4	C5	C6
$\delta_{calculated}$ (ppm)	162.59	115.63	145.07	110.37	145.85	166.73
$\delta_{solid-state}$ (ppm)	155.90	115.60	142.23	114.61	145.15	166.82
$\delta_{D2Osolution}$ (ppm)	154.716	116.116	138.752	112.997	142.674	166.269

of the melted compound. The obtained matter containing the organic entity undergoes decomposition in a wide temperature range [240 to 450°C], too. For all these phenomena several DTA peaks correspond, and a significant weight loss clearly observed on the TGA curve.

This decomposition leads to a black product which contains a residual of organic species mixed with polyphosphoric acids.

IR-Absorption Spectroscopy

The isolated PO_4^{3-} tetrahedron with an ideal T_d symmetry has four vibrational modes: the non-degenerate symmetric stretching mode $\nu_1(A_1)$; the doubly degenerate bending mode $\nu_2(E)$; the triply asymmetric stretching mode $\nu_3(F_2)$; and the triply degenerate asymmetric bending mode $\nu_4(F_2)$. All the modes are Raman active, whereas only $\nu_3$and $\nu_4$are active in the IR. These modes are observed at 938, 420, 1017, and 567 cm^{-1}, respectively.[18,19] The localization of two protons on two oxygen atoms of the $H_2PO_4^-$anion reduces the symmetry from T_d to C_{2V}. Under the effect of its interaction with its crystalline environment

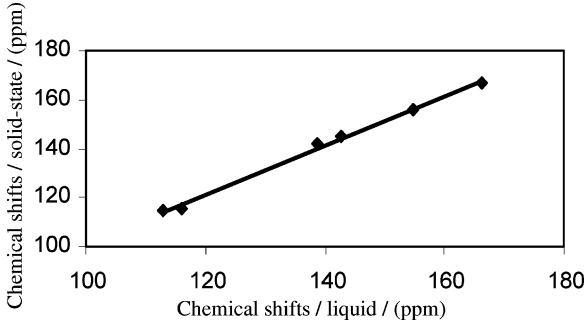

FIGURE 6 Plot of experimental ^{13}C CP-MAS chemical shifts versus chemical shifts in the D_2O solution.

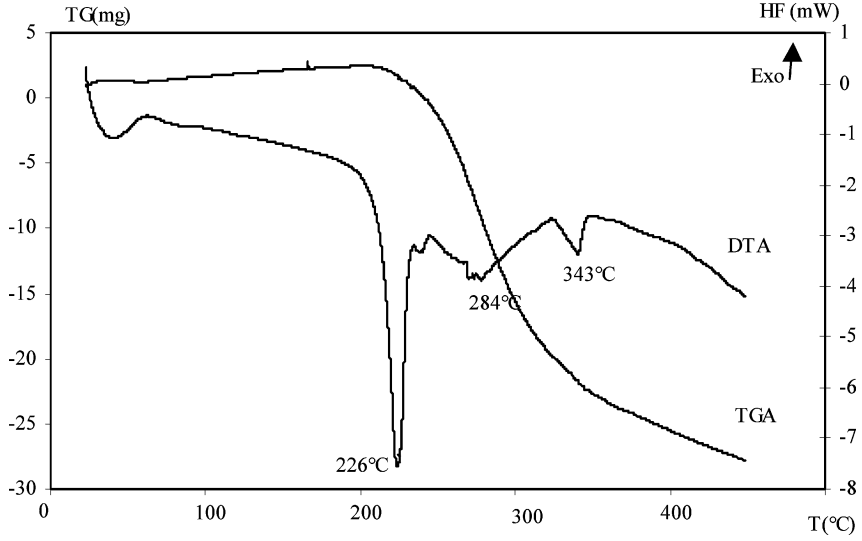

FIGURE 7 DTA and TGA curves of $(6\text{-}NH_2C_5H_3NHCO_2H)H_2PO_4$.

in the studied compound, the $H_2PO_4^-$ anion occupies lower site symmetry C_1. The infrared absorption spectrum of the title compound reported in Figure 8 shows vibrations band characteristic of the organic cation and the $H_2PO_4^-$ anion. The valency vibrations of the organic

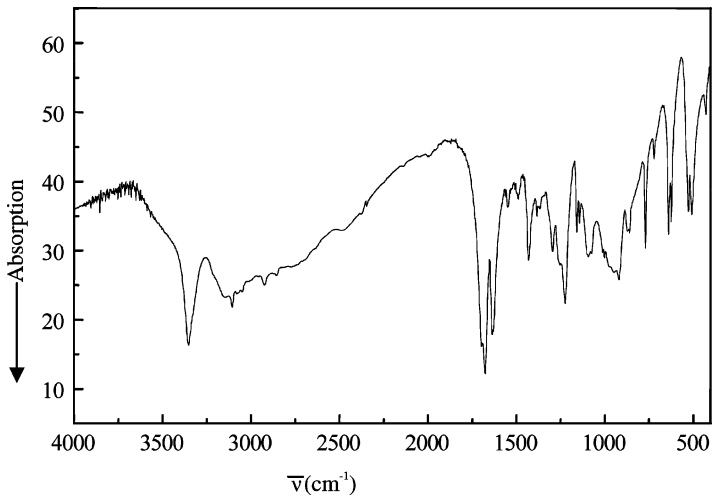

FIGURE 8 Infrared absorption spectrum of $(6\text{-}NH_2C_5H_3NHCO_2H)H_2PO_4$.

group in its protonated form appear between 3400–2500 and 1650–1300 cm^{-1}.[20–21] Various valency and bending vibration bands whose number and positions between 1200 and 300 cm^{-1}, are both characteristic of a monophosphoric anion.[22] In this type of anion, the stretching vibration bands originating from both symmetric $\nu_1(A_1)$ and asymmetric $\nu_3(F_2)$ modes are respectively observed in the range [1000–800] and [1200–1000] cm^{-1} region. The PO_4 tetrahedron has also bending vibration as symmetric $\nu_4(F_2)$ and asymmetric $\nu_2(E)$ respectively observed in the frequency range [650–500] and [500–400] cm^{-1}. The observed shoulder at 1270 cm^{-1}, and the weak band at 825 $cm^{-1}$are assigned respectively to the δ_{P-O-H} in the plane bending and δ_{P-O-H} out of the plane bending modes.[23] The presence of a strong band at 1689 cm^{-1} is assigned to the stretching vibration modes of C=O groups. Multiple bands extending from 3400 to 2500 cm^{-1} are observed in the IR spectrum. These bands must be due to the symmetric and asymmetric stretching modes of NH_2, NH, CH and OH. Frequencies in the range 1700–1300 are attributed to δ(NH), δ(CH) and δ(OH) bending vibrations.

Electrical Conductivity

Conductivity measurements were done on $(6\text{-}NH_2C_5H_3NHCO_2H)\text{-}H_2PO_4$; the resulting complex impedance spectra (-Im. Z (Ω) versus Real Z (Ω)) corresponding to typical examples, recorded at various temperatures are given in Figure 9. The conductivity σ of

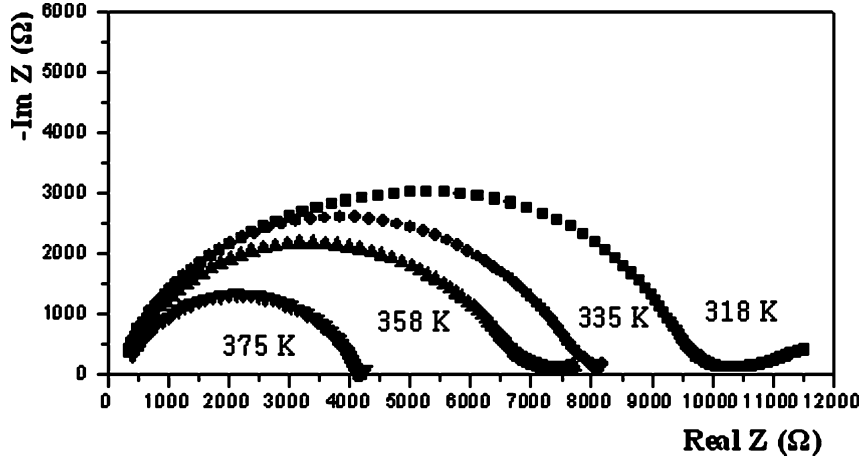

FIGURE 9 Typical impedance spectra of $(6\text{-}NH_2C_5H_3NHCO_2H)H_2PO_4$ at various temperatures.

TABLE IV Conductivity Result Measurement Values

T(K)	R (Ω)	$\sigma(\Omega^{-1}cm^{-1})$	$\ln(\sigma T)$ $(\Omega^{-1}cm^{-1}K)$	$(10^4/T)$ (K^{-1})
318	9714	7.1×10^{-6}	−6.09	31.4
335	7592	9.1×10^{-6}	−5.79	29.8
358	6713	10.3×10^{-6}	−5.60	27.9
375	6532	10.6×10^{-6}	−5.52	26.6
393	6345	10.9×10^{-6}	−5.45	25.4
413	5170	13.3×10^{-6}	−5.20	24.2
430	5013	13.8×10^{-6}	−5.12	23.2
446	4769	14.5×10^{-6}	−5.04	22.4
453	3866	17.8×10^{-6}	−4.82	22.1
466	3574	19.3×10^{-6}	−4.71	21.5

$(6\text{-}NH_2C_5H_3NHCO_2H)H_2PO_4$ was calculated using the following equation $\sigma = d/AR$, where d, A, and R represent the thickness, the area, and the resistance, respectively. The resistance was obtained from the intercept of the Nyquist plot with the real axis. The electrical characteristics (resistance R and conductivity σ) determined for various temperatures, are summarized in Table IV. The temperature dependence of the conductivity between 338 and 466 K is represented in Figure 10 in the form of $\ln \sigma T$ versus $10^4/T$. In this range of temperature, the electrical conductivity increases with increasing temperature. However, the conductivity has approximately an Arrhenius-type behavior $\sigma = A/T \exp(-Ea/KT)$ where A is a constant depending on the material, K the Boltzman

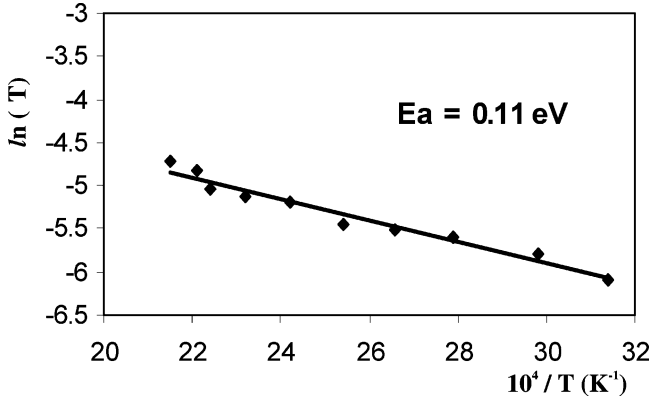

FIGURE 10 Arrhenius plot of the electrical conductivity of (6-$NH_2C_5H_3NHCO_2H)H_2PO_4$.

constant and E_a the activation energy determined by the slope of the interpolating Arrhenius curve ($E_a = 0.11$ eV). This seems to indicate only one protonic conductivity mechanism and there is no modification of the electrical proprieties. These results are in good agreement with the calorimetric study, which does not show any phase transition before the melting point. The electric properties of this hybrid compound may be interpreted by the following way: the rise of temperature can favor the vibration of the inorganic layers, which induce a rapid $H_2PO_4^-$ reorientation and fast H^+ moving.[24] It is worth noting, that these values of electrical conductivity are observed in other phosphate compounds such as $Pb_2Bi(V_{0.84}P_{0.16})O_6$($\sigma_{300K} = 1.3410^{-7}\ \Omega^{-1}cm^{-1}$, $E_a = 0.92$ eV.[25]

CONCLUSION

The use of the protonated 6-aminonicotinic acid as organic cation in the phosphate matrix leads to a new hybrid compound of the chemical formula $(6\text{-}NH_2C_5H_3NHCO_2H)H_2PO_4$. Crystal structure of this compound was found to be built by infinite layers of $H_2PO_4^-$ parallel to the ab plane around $z = 1/2$. Between these layers the organic molecules form chains parallel to the b direction. Both organic and inorganic components perform different interactions (electrostatic, Van der Walls, H—bonds) to stabilize the three—dimensional network. Solid—state ^{31}P and ^{31}C MAS-NMR spectroscopy are in accordance with the X-ray structure.

EXPERIMENTAL

Synthesis of $(6\text{-}NH_2C_5H_3NHCO_2H)H_2PO_4$

The title compound, $(6\text{-}NH_2C_5H_3NHCO_2H)H_2PO_4$, was prepared at room temperature by adding drop by drop (1.03 g, 10.50 mmol) of concentrated monophosphoric acid (85% wt, d = 1.7) to 50 mL of an aqueous solution containing (1.46 g, 10.50 mmol) of 6-aminonicotinic acid ($6\text{-}NH_2C_5H_3NCO_2H$). The mixture was heated at 40°C and stirred to attain homogeneity. Schematically, the reaction can be written as follows:

$$H_3PO_4 + 6 - NH_2C_5H_3NCO_2H \rightarrow (6\text{-}NH_2C_5H_3NHCO_2H)H_2PO_4 \quad (1)$$

The obtained solution was slowly evaporated at room temperature until the formation of short stout prisms of $(6\text{-}NH_2C_5H_3NHCO_2H)H_2PO_4$ (1.5 g, reaction yield 61%), with suitable dimensions for a crystallographic study. The crystals are stable under normal conditions of temperature and humidity.

TABLE V Crystal Data and Experimental Parameters Used for the Intensity Data Collection. Strategy and Final Results of the Structure Determination

Empirical formula	$(6\text{-}NH_2C_5H_3NHCO_2H)H_2PO_4$
Formula weight	236.12
Crystal system	triclinic
Space group	$P\bar{1}$
a	7.221(1) Å
b	8.086(2) Å
c	8.832(5) Å
α	81.97(8)°
β	100.52(8)°
γ	116.32(6)°
Z	2
V	453.4(4) $Å^3$
$\rho_{cal.}$	1.729 $g.cm^{-3}$
F(000)	244
μ (AgK$\bar{\alpha}$)	0.172 mm^{-1}
Crystal size [mm]/Color	0.63 × 0.30 × 0.30 / colourless
Index ranges	$-12 \leq h \leq 12$, $-14 \leq k \leq 14$, $0 \leq l \leq 15$
Reflections collected	4320
Independent reflections	4129
R_{int}	0.011
Refined parameters	170
R[I> 3 σ(I)]	0.030
$R_{(w)}$	0.050
Goodness-of-fit	1.350

Investigation Techniques

X-ray Diffraction

The intensity data collection was performed with a Mach3 Enraf Nonius diffractometer. The experimental parameters used during these measurements, the strategy followed for the structure determination and its final results are gathered in Table V.

Crystallographic data (CIF) for the structure reported in this article have been deposited with the Cambridge Crystallographic Data Center CCDC as supplementary publication No.294276. Copies of the data can be obtained, free of charge, on application to the CCDC, 12 Union Road, Cambridge CB12EZ, UK (Fax: +44(1223)336-033; e-mail: deposit@ccdc.cam.ac.uk).

NMR Spectroscopy

^{31}P MAS-NMR and ^{13}C CP MAS-NMR spectra were obtained on a solid-state high-resolution Bruker DSX-300 spectrometer operating at

121.51 MHz for ^{31}P and 75.49 MHz for ^{13}C. ^{31}P NMR chemical shifts are given relative to 85% H_3PO_4 and ^{13}C ones relative to tetramethylsilane as external reference.

^{13}C spectrum of the sample dissolved in D_2O solution was recorded on a Bruker DSX-300 spectrometer. Tetramethylsilane (TMS) was used as a reference agent.

Thermal Analysis

Thermal analysis was performed using the "multimodule 92 Setaram analyzer" operating from room temperature up to 723 K at an average heating rate of 5 K min^{-1}.

Infrared Spectroscopy

IR spectrum is recorded in the range 4000–400 cm^{-1} with a "Perkin-Elmer FTIR" Spectrometer using a sample dispersed in a spectroscopically-pure KBr pellet.

Electrical Conductivity

Under 12-ton pressure, a polycrystalline sample of $(6\text{-}NH_2C_5H_3NHCO_2H)H_2PO_4$ was crushed and pressed at room temperature into a 13-mm diameter tablet with a 0.92-mm thickness. Dense pellets suitable for electrophysical measurements were heated at 323 K for 24 h. After heating, the pellets were checked by X-ray powder diffraction, which showed that material is chemically stable in this range of temperature. Metallic silver was deposited on both sides which served as electrodes. The pellet is placed between two blocking electrodes in a tubular furnace, submitted to a temperature regulator.

The electrical conductivity measurements were carried out from 318 K to 466 K with 5–20 K steps, by checking the complex impedance spectroscopy with a Hewlett-Packard 4129A impedance analyzer. The signal frequency ranged from 10 Hz to 13 MHz.

REFERENCES

[1] G. L. Wilkes, B. Orler, and H. Huang, *Polym. Prepr.,* **26,** 300 (1985).
[2] R. Masse, M. Bagieu - Beucher, J. Pecaut, J. P. Levy, and J. Zyss, *Nonlinear Opt*., **5,** 413 (1993).
[3] M. Gatti, G. Ferraris, and S. A. Masson, *Acta Cryst.,* **B36**, 254 (1980).
[4] A. J. Wright and J. P. Attfield, *J. Solid State Chem.*, **141,** 160 (1998).
[5] A. J. Wright and J. P. Attfield, *Inorg. Chemistry*, **37,** 3858, (1998).
[6] W. H. Baur, *Acta Cryst*., **B30,** 1195 (1974).
[7] M. T. Averbuch-Pouchot, A. Durif, and J. C. Guitel, *Acta Cryst.*, **C44,** 1968 (1988).
[8] B. Back, L. Hansen-Nygaard, and J. Rastrup-Andersen, *J. Mol. Spectrosc*., **2,** 361 (1958).

[9] C. Janiak, *J. Chem. Soc.*, *Dalton Trans.*, 3885 (2000)
[10] H. Dhaouadi, H. Marouani, and M. Rzaigui, *Z. Kristallogr.*, NCS **220,** 433 (2005)
[11] A. Chtioui and A. Jouini, *Mater. Res. Bull.,* **41,** 569 (2005)
[12] A. R. Grimmer and U. Haubenreisser, *Chem. Phys. Lett.*, **99,** 487 (1983).
[13] D. Mûller, E. Jahn, G. Ladwig, and U. Haubenreisser, *Chem. Phys. Lett.,* **109,** 332 (1984).
[14] A. K. Cheetham, N. J. Clayden, C. M. Dobson, and R. J. B. Jakemen, *J. Chem. Soc. Chem. Commun.*, **4**, 195 (1986).
[15] L. Mudracovskii, V. P. Shmochkova, N. S. Kentsarenko, and V. M. Mastikhin, *Phys. Chem. Solids*, **47,** 335 (1986).
[16] G. L. Turner, K. A. Smith, R. J. Kirkpatrick, and E. J. Oldfield, *Magn. Reson.*, **70,** 408 (1986).
[17] S. Prabhakar, K.J. Rao, and C. N. R. Rao*, Chem. Phys. Lett.,* **139,** 96 (1987).
[18] K. Nakamoto, *IR and Ra Spectra of Inorganic and Coordinate Compounds* (Wiley-Interscience, New York, 1986).
[19] E. Steger, K. Herzog, and Z. Anorg., *Allogo. Chem.,* **331,** 109 (1964).
[20] A. Gharbi, A. Jouini, M. T. Averbuch-Pouchot, and A. Durif, *J. Solid State Chem.,* **111,** 330 (1994).
[21] D. Dolphin and A. E. Wick, *Tabulation of Infrared Spectra Data* (John Wiley and Sons, New York, 1977).
[22] S. Kammoun, M. Kammoun, A. Daouad, and F. Romain, *Spectrochim. Acta Cryst.*,**47A,** 1051 (1991).
[23] A. C. Chapman and L. E. Thirlwell, *Spectrochim. Acta*, **20,** 937 (1964).
[24] A. Schechter and R. Savinell, *Solid State Ionics,* **147,** 181 (2002).
[25] O. Labidi, P. Roussel, M. Huve, M. Drache, P. Conflant, and J. P. Wignacourt, *J. Solid State Chem.*, **178,** 2247 (2005).